THE PRODUCTION AND MEASUREMENT OF 150 PS BEAM PULSES FROM THE TRIUMF CYCLOTRON

W.R. Rawnsley, G.H. Mackenzie, C.J. Oram
TRIUMF, 4004 Wesbrook Mall, Vancouver, B.C., Canada V6T 2A3

Summary

A microchannel plate (MCP) with a 50 Ω anode has been used to confirm predictions that TRIUMF's phase restricting slits produce beam pulses 0.15 ns wide (1.3° RF). A 194 MeV extracted beam of a few nA passed through a thin, 25 μm, aluminum foil. X-rays from the foil were detected by the MCP mounted 177 mm away. A 110 gaussmeter field between target and channel plate swept all electrons out of the 3 msr acceptance. The MCP was followed immediately by a TRIUMF x 10 hybrid amplifier. The output was taken to standard nucleonics over 36 m of FM-8 cable. The discriminated MCP pulses started a TAC, and the stop was derived from the cyclotron RF. The count rate was ~500/nA. The current through the cyclotron slits was equivalent to ~5 μA. Several estimates on our narrowest cyclotron tune indicate that the measured 158 ps FWHM is made up from a 140 ps beam contribution and 73 ps from the electronics. The device will be used to explore the sources of cyclotron instabilities and to provide a low current, cyclotron independent, time pick-up for the experimental program.

Introduction

The TRIUMF H^- cyclotron has a low central field, B_c = 3 kG, a fairly large energy gain of 0.3 MeV per turn and the RF accelerating frequency (23 MHz) is a fifth harmonic of the ion orbit frequency. The combination of a large radius gain per turn of 15 mm at 30 MeV together with a rapid variation of particle radius with RF phase make it possible for a system of flags and slits to define a beam of narrow phase width, say ±2° RF, while accepting much of the beam injected into that narrow interval.[1]

Internal current patterns taken at low energies are consistent with these narrow phase acceptances, however, until recently it has been difficult to measure these time widths in an extracted beam of several hundred MeV since the intrinsic resolution of standard scintillators and photomultipliers is about 0.3 ns. Microchannel plates (MCP) have made available high gain electron multiplication with a very small intrinsic time spread[2] (less than 80 ps) and are sensitive to particles that can be produced by direct interactions. These include secondary emission and low energy knock-on electrons and X-rays. These particles have high production cross-section and extremely thin foils can be used to interact with the primary beam and produce an adequate flux. This is important since the device will eventually be used in conjunction with experiments and any foil placed upstream of an experimental target degrades the beam quality. MCP detection efficiency for electrons up to 2 keV is about 80% falling to 10% for 50 keV electrons and with lower efficiency for still higher energies. The detection efficiency for 1 to 10 keV X-rays ranges from 7 to 3%.[3] Although the time resolution is narrow the spread in pulse height produced for a monoenergetic incoming beam of electrons or X-rays is broad.

The coefficient for the production of low energy electrons in an aluminum foil ranges from 5% per surface at 200 MeV to about 3% per surface at 500 MeV, the MCP will receive electrons from one surface only. The production is homogenous in space. The energy of K-shell X-rays from aluminum is approximately 1.5 keV. The production cross-sections from protons in this energy range are 6.7×10^3 barns with an additional contribution from energetic delta rays of about 30%.[4] It should be noted that the total nuclear reaction cross-section for proton induced reactions is about 0.4 barns. The X-ray distribution will be homogeneous at a rate of 1.3 X-rays per proton for a 25 μm aluminum foil, however, most of these X-rays will not escape from the foil since the absorption mean free path is about 3 μm. This reduces the X-ray rate somewhat below the electron rate. An uncollimated 25 mm diameter MCP 177 mm from the beam spot would accept 10^{-3} of the particles produced which would be a rate of 7.5×10^6 per proton multiplied by the production coefficient and the detection efficiency leading to a count rate of 10^4 to 10^5 per nanoamp depending on additional collimation and discrimination.

The equipment and techniques used to define, in the cyclotron, a beam of good quality are described in Ref. 5. In brief, the beam injected into the cyclotron is prebunched into a width of 2.5 ns FWHM (20° RF). An initial phase selection is made by a flag on the first turn which eliminates the more extreme positive or negative phases. A second slit operating on usually the sixth turn produces a further phase restriction to ±5°. A series of electrostatic plates are used to minimize the vertical coherent amplitude and a vertical flag controls the size of the vertical incoherent amplitude; this is used to reduce the amount of coupling between vertical and radial planes during acceleration. A first harmonic coil minimizes the radial coherent amplitude and a final set of 3 slits operating between 15 and 30 MeV control the radial emittance and further define the phase width. Differential probe scans at 70 MeV are consistent with the radial emittance and phase width expected. However, the time averaged phase widths may be broadened during acceleration to the extraction energy by machine instabilities, such as deviations in average field or accelerating frequency from their isochronous values. The absolute number of turns made to the point of extraction is less important provided that variations in, for example, V_{peak} are not so large as to alter the central phase selected by the slits.

Experimental Arrangement

A Galileo Electro-Optics Corporation MCP model FTD 2002 was used. It was a 2.5 cm diameter, 25 μm bore, chevron type with an 8° bias angle and had a 50 Ω anode with a General Radio connector (Fig. 1). An adapter was built into a 4" Marmon flange to pass the signal

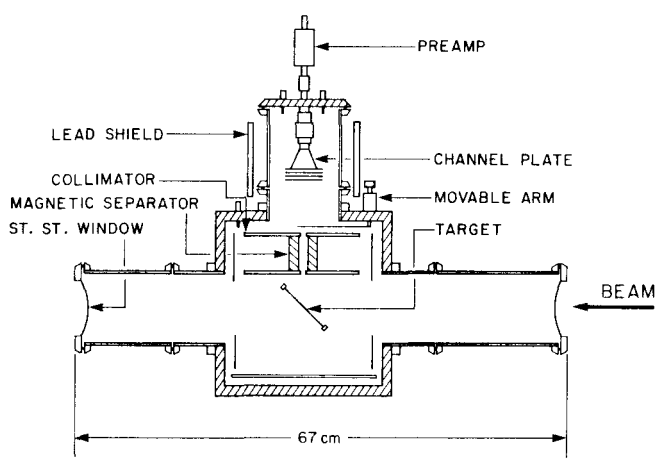

Fig. 1. The test apparatus. The microchannel plate assembly is mounted above a thin foil target.

CH1996-3/84/0000-0237 $1.00 © 1984 IEEE

through a BNC vacuum feedthrough. The adapter provided a very short non-reflecting signal path in addition to mechanical support for the MCP assembly while the flange allowed removal and handling. The MCP was mounted in a 4" length of 4" diameter beam pipe on the top plate of a standard TRIUMF 10" vacuum box for most of the tests. A moveable arm, suspended from a rotary ferrofluidic feedthrough, was used to swing a particle source or absorber in front of the MCP. The target for the proton beam experiments was a fixed 7 mg/cm^2 aluminum foil held at 45° to the MCP and beam.

The MCP required a vacuum of at least 10^{-5} Torr to prevent excessive ion feedback. 3×10^{-7} to 10^{-6} Torr was achieved with a 450 l/s turbo pump. 25 μm stainless steel vacuum windows were placed about 30 cm up and down stream from the target to reduce the background from scattered beam.

The monitor box was positioned at an achromatic double focus in beam line 4B, Fig. 2. The majority of measurements were made at 200 MeV. Beam optics calculations, TRANSPORT code, indicate that, for the emittance and momentum spread expected, the 2 cm long beam pulse would lengthen by 5% between the extraction foil and MCP target. This does not affect MCP use for cyclotron diagnostics. An attempt was made to calculate a beam line tune that would shorten the pulse and test MCP and electronic resolution; however, the TRANSPORT code was unable to find a solution that did not cause large increases in transverse beam size.

A Bertan 1792N power supply with fast over current trip provided high voltage bias for the MCP. A resistive divider network with low voltage test points was adjusted to equalize the voltages across the plates. The anode was operated close to ground potential to facilitate signal coupling.

The MCP signal was amplified immediately by a fast × 10 hybrid circuit mounted on the vacuum feedthrough. The signal was brought out of the beam line area by 36 m of FM-8 cable (Fig. 3). A Lecroy 825Z discriminator provided a timing pulse while two more discriminators formed a level sensitive window in which the larger pulses were accepted (Fig. 4); this minimises "walk". These pulses started an ORTEC 476 time to amplitude converter (TAC). The 23 MHz sine wave from the cyclotron RF resonator pick- up was discriminated and used as the stop signal. An 8 μs long busy signal from the TAC vetoed MCP after-pulses due to ion feedback, and eliminated electronic pile-up. The TAC output could be observed using a multichannel analyzer (MCA) at the electronics rack or in the cyclotron control room. The time per channel was calibrated by introducing known delays into the sine wave portion of the RF signal path. The beam line polarimeter rate was used to determine the primary proton beam intensity.

Commissioning

Electron Measurements

Channel plate and amplifier operation were bench checked using a 100 μCi Ru^{109} beta source mounted on the moveable arm. The initial beam measurements were made detecting secondary electrons. An apparatus similar to that shown in Fig. 1, but with a wide aperture electrode in place of the collimator, was used. The count rate was very high, about 5×10^5/nA. The time spectrum of the MCP pulses had a sharp 200 ps leading edge followed by a flat top and a long 4 ns tail. Independent power supplies were used to vary the target and electrode voltages from plus to minus 3 kV but had little effect on the count rate and spectrum shape. It was concluded that the sharp leading edge was due to photons while the tail was the result of secondary electrons of many energies. To avoid the use of an

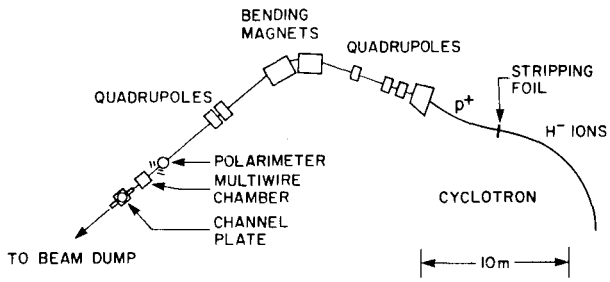

Fig. 2. The low current proton beam line 4B used for the tests.

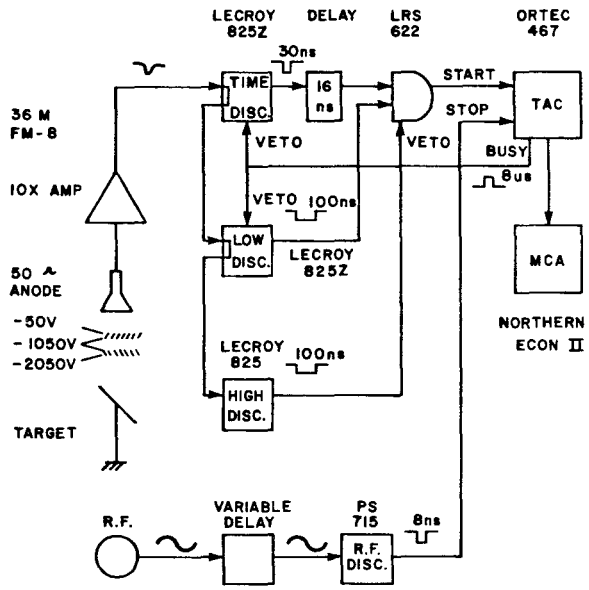

Fig. 3. Schematic of the electronics. Standard modules produced time spectra with respect to the cyclotron RF.

accelerating grid (which would have caused additional beam scattering) to monochromatize the electrons we decided to eliminate them and observe X-rays.

X-ray Measurements

The sweeping magnet shown in Fig. 1, with field 2.2 kG over 5 cm and entrance and exit collimator holes

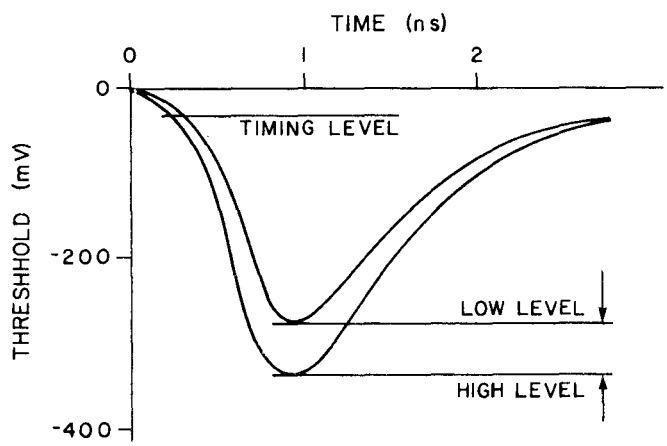

Fig. 4. The pulse discrimination system uses three thresholds. The gate between high and low levels selects fast rising pulses.

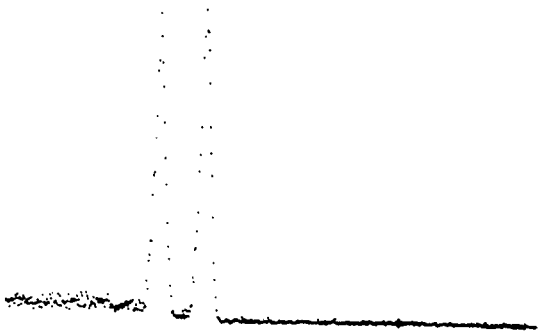

Fig. 5. A typical spectrum using scattered X-rays. A 1 ns calibration delay separates the two traces.

of diameter 6.35 mm and 9.5 mm, respectively, was installed. Particles with $H\rho$ less than 63 kG cm no longer reached the MCP. This included all electrons with energies of less than 18.5 MeV and protons with energies of less than 0.19 MeV. The width of the time spectrum was immediately improved to 1 ns or less. The tails remaining were removed by the installation of a lead collar 10 mm thick placed around the MCP to screen it from particles produced far upstream by the beam halo interacting with the beam pipe. Following adjustment to the cyclotron magnetic field the peak width now fell in the expected range of a few hundred ps as seen in Fig. 5. A 50 μm aluminum absorber could be

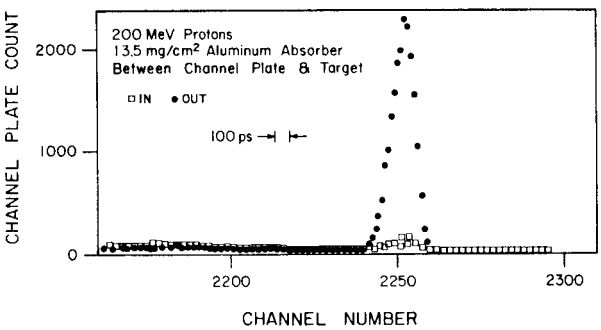

Fig. 6. The effect of a 50 μm aluminum absorber foil on the detecced particles.

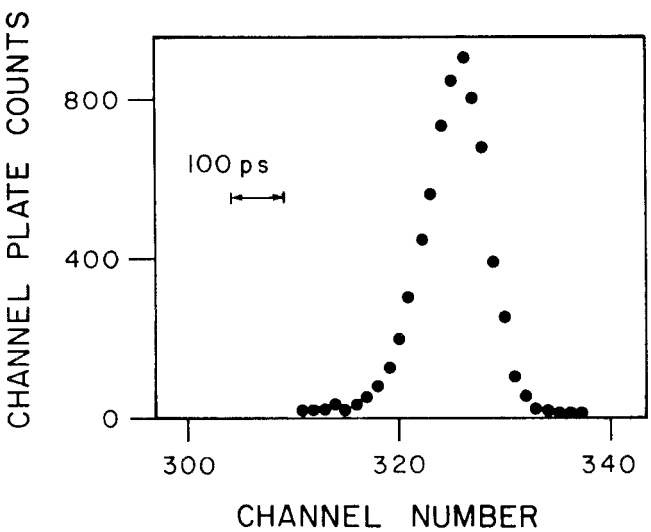

Fig. 7. A typical time spectrum for the case where the cyclotron magnetic field was slightly out of isochronism allowing the slits to select a narrow phase.

inserted between the collimator and MCP and as seen in Fig. 6 this eliminated almost the entire peak confirming again that the MCP was counting X-rays.

The voltage across each chevron was increased from 925 to 1100 V. The FWHM and peak channel did not vary significantly, though the count rate increased as more pulses reached the low discriminator level.

The MCP count rate was observed as the beam was steered horizontally and then vertically across the target to confirm that the collimator acceptance included most of the beam spot. The geometry would accept particles from a 9.9 mm wide by 9.2 mm high ellipse. The peak of the time spectrum indicated a reduction in the time of flight of 4.1 ± 1.5 ps/mm as the beam was steered upward. The effect was the result of the lengthening of the path for protons approaching the target at velocity βc and the reduction of the path for photons leaving it at velocity c. For 200 MeV protons the calculated value is 2.6 ps/mm implying an effective broadening of 24 ps for a beam occupying the entire vertical acceptance of the target.

The discriminator gate width was varied while keeping it centred on 308 mV. We found that the MCP count rate was proportional to the gate width and that the observed FWHM approached 190 ps as the gate width approached zero (Fig. 8). This allowed us to estimate the electronic contribution to the FWHM assuming it was a linear function of the gate width. Electronic jitter was also studied with a 1 ns risetime pulse generator in place of the MCP and the FWHM was again seen to be proportional to the gate width. Assuming that the MCP contributes a negligible fraction of the observed width then:

$$\text{FWHM(elec)} = 2.19 \text{ ps/mV} \times \text{gate width (mV)} \qquad (1)$$

$$\text{FWHM(beam)}^2 = \text{FWHM(observ)}^2 - \text{FWHM(elec)}^2 \qquad (2)$$

The FWHM(beam) was calculated and plotted as a function of gate width in Fig. 8. An average FWHM(beam) of 173 ± 10 ps was obtained with a chi squared of 5.25 for the 5 degrees of freedom. This is probably a slight overestimate of the FWHM of the beam because any contribution from the MCP will reduce this number.

Figure 7, with a FWHM of 158 ps, was obtained using a gate width of 33 mV. Equations 1 and 2 indicate an electronics contribution of 73 ps and a beam contribution of 140 ps.

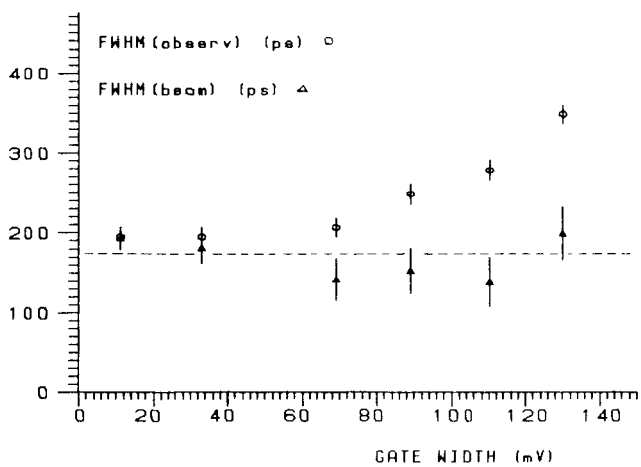

Fig. 8. The effect of discriminator gate width on the measured FWHM and the calculated FWHM of the beam.

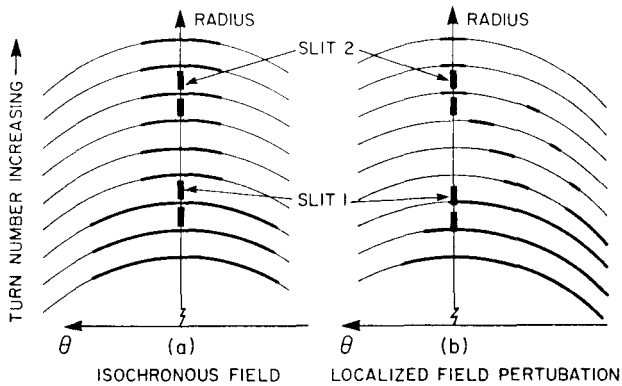

Fig. 9. Schematic representation of the use of slits to reduce the phase width of the beam being accelerated.

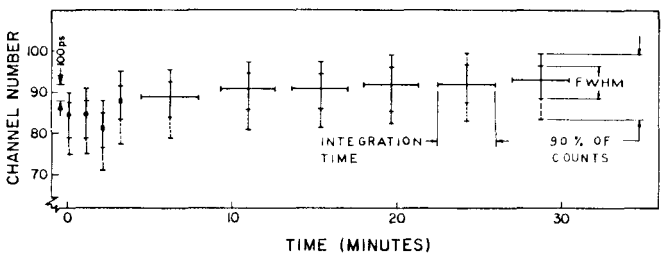

Fig. 10. Stability run. The short term and long term stability of the time spectra is evident.

Cyclotron Experiments

In general the cyclotron is tuned to deliver the maximum current within a given energy spread, i.e. within a given incoherent radial amplitude, A_i, determined by the slit width. Under these conditions the central beam phase at the slit radius is 0°, the turn width is a minimum and the phase band transmitted a maximum. A typical MCP spectrum under these conditions is given in Fig. 5. When trim coils are adjusted to detune the magnetic field the central phase slips from 0° and the turn width broadens. If the slit radius only is re-adjusted a beam of reduced intensity is selected with the same A_i but a narrower phase width, see Fig. 9. Beam prepared with this technique was used to obtain the data in Figs. 7 and 10.

Cyclotron stability was investigated as shown in Fig. 10. The first four spectra, accumulated for 9 seconds each, indicated a peak channel RMS jitter of 58 ps over 4 minutes. This is probably due to short term RF resonator instability. The following six spectra, accumulated for 3.5 minutes each, had a peak channel drift of 93 ps over 22 minutes. The FWHM for all spectra remained essentially constant at 198 ps with a slightly sharper leading than trailing edge, a characteristic of the particular cyclotron tune. The drift of the peak channel would effectively broaden the FWHM integrated over 22 minutes by 29 ps.

A second estimate of the relative contribution of beam width and instrumental noise may be made by quantitatively adjusting the magnetic field at the extraction radius to move the central phase between, say, -60° and +60°. Since the number of turns to the extraction radius is altered the beam must be well

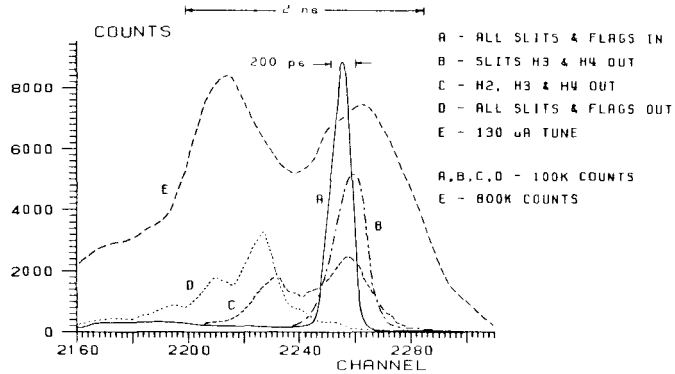

Fig. 11. The effect of the removal of the phase limiting slits and flags.

centered to maintain the extracted energy and to avoid phase-energy correlations. The predicted phase slip may be confirmed from the movement of the MCP peak with respect to the RF. Since $\Delta\sin\phi$ is preserved in this operation, not $\Delta\phi$, the width of the beam contribution will increase as $1/\cos\phi$. Using eq. (2) we again infer that the instrumental contribution is less than the beam width at the target.

Figure 11 shows the increase in time width as the beam defining slits and flags were withdrawn in the reverse order from their sequential insertion described above. As the devices are withdrawn the circulating beam intensity rises and the foil must be raised, sampling less of the beam, to maintain a safe current in BL4B. In addition the phases previously stopped will, in general, be accelerated off-centre altering the mean extracted energy. The data for 130 μA circulating was obtained after several hours of re-optimisation. The fine structure varies with time due to machine instabilities and is somewhat emphasized since the BL4B foil was extracting from the halo.

Future

New discriminators (Phillips Scientific) have been ordered. A MCP with a retractable target is being designed for permanent installation in the vault section of the proton area beam lines. It will be used for cyclotron diagnostics including cyclotron stabilization work and as a general timing reference for the experimenters. In particular, the MCP's ability to detect narrow beam pulses will make it useful as a start signal for neutron time-of-flight experiments and beam energy measurement.

We would like to thank J.V. Cresswell for advice and loan of the hybrid amplifier and the technicians of the Technology Division and the Probes group for help in assembly and installation of the apparatus.

References

1. C. Kost and G.H. MacKenzie, TRIUMF design note TRI-DN-73-18 (1973).
2. J. Girard and M. Bolore, NIM 140 (1977) 279.
3. J.L. Wiza, NIM 162 (1979) 587.
4. O.N. Jarvis, C. Whitehead, M. Shah, Phys. Rev. 5 (1972) 1198.
   K.W. Jones, private communication (1983).
5. G.H. Mackenzie et al., IEEE NS 26, 3218, 1979 (Fig. 1).